AIP | Journal of Applied Physics

Phase transformations in multiferroic Bi1− x La x Fe1− y Ti y O3 ceramics probed by temperature dependent Raman scattering

L. P. Xu, L. L. Zhang, X. L. Zhang, J. Z. Zhang, Z. G. Hu, J. Yu, and J. H. Chu

Citation: Journal of Applied Physics **116**, 164103 (2014); doi: 10.1063/1.4900439
View online: http://dx.doi.org/10.1063/1.4900439
View Table of Contents: http://scitation.aip.org/content/aip/journal/jap/116/16?ver=pdfcov
Published by the AIP Publishing

Phase transformations in multiferroic $Bi_{1-x}La_xFe_{1-y}Ti_yO_3$ ceramics probed by temperature dependent Raman scattering

L. P. Xu (徐丽萍),[1] L. L. Zhang (张林林),[2] X. L. Zhang (张小龙),[1] J. Z. Zhang (张金中),[1] Z. G. Hu (胡志高),[1,a)] J. Yu (于剑),[2] and J. H. Chu (褚君浩)[1]
[1]*Key Laboratory of Polar Materials and Devices, Ministry of Education, Department of Electronic Engineering, East China Normal University, Shanghai 200241, China*
[2]*Functional Material Research Laboratory, Tongji University, Shanghai 200092, China*

(Received 6 July 2014; accepted 14 October 2014; published online 27 October 2014)

Optical phonons and phase transitions of $Bi_{1-x}La_xFe_{1-y}Ti_yO_3$ (BLFTO, $0.02 \le x \le 0.12$, $0.01 \le y \le 0.08$) ceramics have been investigated by Raman scattering in the temperature range from 80 to 680 K. Four phase transitions around 140, 205, 570, and 640 K can be observed. The Raman modes are sensitive to the spin reorientation around 140 and 205 K, owing to the strong magnon-phonon coupling. The transformation around 570 K is a structural transition from rhombohedral to orthorhombic phase due to an external pressure induced by the chemical substitution. The anomalies of the phonon frequencies near Néel temperature T_N have been discussed in the light of the multiferroicity. Moreover, it was found that the structural transition temperature and T_N of BLFTO ceramics decrease towards room temperature with increasing doping composition as a result of size mismatch between substitution and host cations. © *2014 AIP Publishing LLC*.
[http://dx.doi.org/10.1063/1.4900439]

I. INTRODUCTION

$BiFeO_3$ (BFO) has been hailed as an important material for magnetoelectric devices due to its room-temperature (RT) multiferroic properties, in which the electric polarization is coupled to antiferromagnetic (AFM) order, allowing for manipulation of magnetism by applied electric fields and vice versa.[1–4] BFO ceramics possess a rhombohedrally distorted perovskite structure with space point group *R*3c at RT. This phase shows a spontaneous polarization along the $[111]_{pseudocubic}$ threefold polar axis and antiphase FeO_6 rotations around the same axis, corresponding to (a^- a^- a^-) tilt system in Glazer's notation.[5] The Fe^{3+} magnetic moments are arranged in a cycloidal type of periodicity 62 nm, incommensurating with the lattice and superimposed on a slightly canted *G*-type antiferromagnetic order.[6] BFO is antiferromagnetic below Néel temperature ($T_N = 643$ K) and ferroelectric below Curie temperature ($T_C = 1103$ K).[7]

However, BFO is often associated with impurities and compositional instabilities.[8,9] A potential route for moderating these problems is substitution on the Bi and/or Fe sites. In addition, element substitution can destroy the cycloidal spiral structure that prohibits a macroscopic first-order magnetoelectric coupling.[8] Due to the absence of cycloidal spin order induced by doping, linear magnetoelectric effects in the noncentrosymmetric phases of doped BFO ceramics become symmetry allowed, which is motivated by a coupling between the *A*-site ferroelectric translation and *B*-site magnetization through the antiferrodistortive (a^- a^- a^-) tilt of the oxygen octahedra.[10] The *A*-site (Bi-site) substitution by La^{3+} can enhance the ferromagnetic property of BFO.[6,11,12] Apart from the substitution on the *A*-site, *B*-site (Fe-site) substitution can stabilize enhanced ferromagnetic and magnetoelectric coupling interaction. For example, Fe-site substitution by Ti^{4+} can reduce the oxygen vacancies significantly due to the requirements of charge compensation, which can minimize associated leakage current. Moreover, the hybridization between Ti 3*d* and O 2*p* states is essential for stabilizing the ferroelectric distortion.[11,13,14] Thus, La and Ti codoped BFO can combine the advantages of separate contribution, such as enhanced compositional stability, improved ferromagnetic properties, and reduced leakage current.

During the last several years, intriguing behavior was found in doped BFO compounds.[15–18] A single phase transition from *R*3c to *Pnma* structure was reported in $Bi_{1-x}La_xFeO_3$ ceramics around $x = 0.18$.[15] A similar structural transition from *R*3c to *Pbam* was also observed from $Bi_{1-x}Nd_xFeO_3$ system around $x = 0.15$, which transforms into nonpolar *Pnma* on heating slightly above 573 K.[16] In addition, substitution on the *B*-site introduces another source of structural distortion.[17] Recent X-ray diffraction data on the $Bi_{0.9}Sm_{0.1}Fe_{1-x}Mn_xO_3$ series show a complicated transition from *R*3c to an incommensurate structure via *Pnam* phase.[18] Motivated by the intriguing behaviors in reported structural data as well as a general lack of detailed structural study on La and Ti codoped BFO ceramics, we present Raman results on $Bi_{1-x}La_xFe_{1-y}Ti_yO_3$ (BLFTO, $0.02 \le x \le 0.12$, $0.01 \le y \le 0.08$) to systematically study phase transitions induced by the chemical substitution and temperature. Generally, Raman scattering as a nondestructive technique possesses strong selection rules. Furthermore, Raman spectroscopy is known to be a powerful technique for the investigation of even subtle structural distortions both within a space group (via band shifts) and due to a phase transition (via band splitting and/or soft modes etc.). The phonon mode patterns can be explained by the variations of frequency,

a)Author to whom correspondence should be addressed. Electronic mail: zghu@ee.ecnu.edu.cn. Tel.: +86-21-54345150. Fax: +86-21-54345119.

intensity, and full width at half maximum (FWHM) by means of the spectral analysis. Especially, the phonon frequencies as a function of temperature could be a crucial tool to investigate phase transition.[19–21]

In this work, phase transitions of BLFTO ceramics have been investigated by temperature-dependent Raman spectroscopy. Three magnetic phase transitions around 140, 205, and 640 K are observed. Especially, a structural transition from rhombohedral to orthorhombic phase has been found around 570 K. Moreover, composition dependence of phase transition temperatures and La/Ti codoping effects have been discussed in detail.

II. EXPERIMENTAL DETAILS

BLFTO ceramics were prepared by a traditional solid state reaction method with Bi_2O_3 (Alfa Aesar 99%), Fe_2O_3 (Alfa Aesar 99.945%), La_2O_3 (Sinochemical 99.99%), and TiO_2 (Acrōs 98%) as raw materials.[22] In order to remove the surface overlayer artifacts in analyzing the Raman data, all BLFTO wafers were double-side polished with a mechanical polishing progress. Temperature dependent Raman spectra were collected with a Jobin-Yvon LabRAM HR 800 micro-Raman spectrometer and a THMSE 600 heating/cooling stage (Linkam Scientific Instruments) in the temperature range from 80 to 680 K with a resolution of 0.1 K. A laser with the wavelength of 633 nm was used as the excitation source and the spectral resolution is better than 1 cm^{-1}. The laser beam was focused through a 50× microscope with a working distance of 18 mm. An air-cooled charge coupled device (CCD) was used to collect the scattered signal dispersed on 1800 grooves/mm grating in the frequency range of 10–700 cm^{-1}. In order to study the variation trend of phonon modes, Raman spectra were fitted with independent damped harmonic oscillators. The crystal structure was analyzed by x-ray diffraction (XRD) using Cu Kα radiation (D/MAX-2550 V, Rigaku Co.).

III. RESULTS AND DISCUSSION

Fig. 1(a) depicts room-temperature XRD patterns of the BLFTO ceramics. A single rhombohedral phase (*R*3c) is obtained up to the doping composition of $x = 0.10$ and $y = 0.06$. With increasing doping compositions of La and Ti, the intensity of (006) and (118) diffraction peaks decrease gradually. As shown in the inset of Fig. 1(a), the intensity of (104) peak reduces while the intensity of (110) peak increases and finally they merge into a single broad peak with a shift towards higher angles near $x = 0.12$, $y = 0.08$, indicating the appearance of orthorhombic (*Pbam*) phase. The absence of (104) diffraction peak clearly suggests a mixed structure state with a dominant (*R*3c) phase.[8]

The Brillouin zone center normal modes of BFO, which possess a rhombohedrally distorted perovskite structure with space point group *R*3c, can be classified into $4A_1 \oplus 5A_2 \oplus 9E$ irreducible representations. The $4A_1$ and the doubly degenerate $9E$ modes are simultaneously infrared (IR) and Raman active, while the A_2 modes are nonpolar and silent. Fig. 1(b) shows Raman spectra of the BLFTO ceramics at 80 K. All spectra were corrected for the Bose-Einstein temperature factor to facilitate comparison and eliminate the contribution from the Bose Einstein population factor. Raman spectra, which are consistent with the *R*3c structure, are visible up to the composition of $x = 0.10$, $y = 0.06$. Some remarkable differences could be observed as the values of x and y increase. The phonon modes become weaker and broadening as La and Ti compositions increase. The most obvious one is the peak at 175 cm^{-1}. In BFO, Bi atoms only take part in low-frequency modes below 167 cm^{-1} while oxygen motion is mainly involved in modes above 262 cm^{-1}. Fe atoms strongly dominate in the modes between 152 and 262 cm^{-1} but also make contribution to some higher-frequency modes.[23] It is natural that the intensity of the relevant modes declines with the La and Ti substitution. The peaks at 74, 139, and 240 cm^{-1} gradually disappear with increasing doping compositions of La and Ti, demonstrating that the rhombohedral distortion of BFO is inhibited. The appearance of the peak at 50 cm^{-1} near the composition of $x = 0.12$, $y = 0.08$ indicates that the antiferroelectric (AFE) *Pbam* type structure begins to emerge. The variation trends observed from Raman spectra agree well with those derived by the XRD data. The obtained peak positions for all

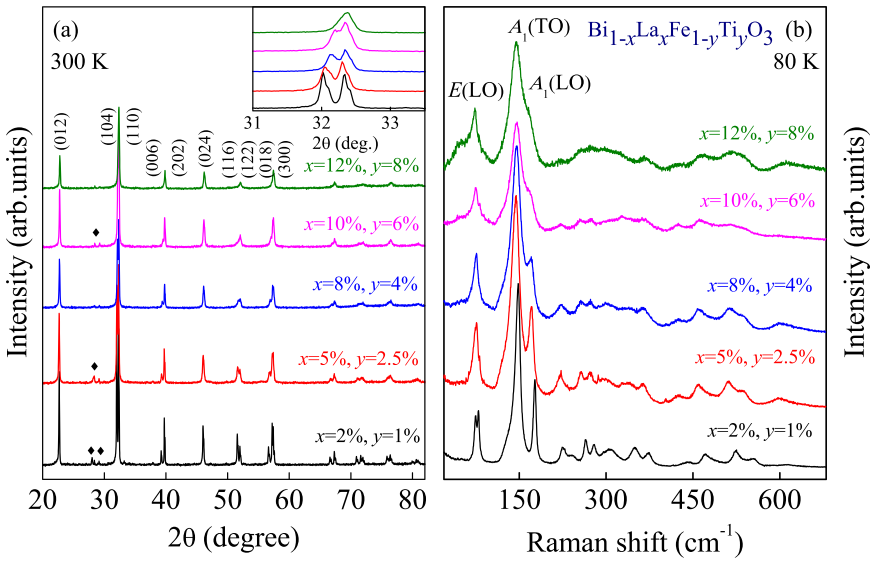

FIG. 1. (a) The XRD patterns of BLFTO ceramics at room temperature. Peaks from the impurity phase $Bi_2Fe_4O_9$ are indicated by the symbol "◆." The inset shows the enlarged region around $2\theta = 32°$. (b) Raman spectra of the BLFTO ceramics recorded at 80 K and the mainly corresponding assignments have been remarked.

TABLE I. The phonon frequencies and the symmetry assignments of the BLFTO ceramics (in cm^{-1}, at 80 K).

Phonon mode	$x=0.02$, $y=0.01$	$x=0.05$, $y=0.025$	$x=0.08$, $y=0.04$	$x=0.10$, $y=0.06$	$x=0.12$, $y=0.08$
A_1(TO)	…	…	…	…	51
E(TO)	74	74	70	…	…
E(LO)	79	78	77	75	74
E(TO)	139	138	137	…	…
A_1(TO)	148	148	149	149	148
A_1(LO)	176	175	174	172	170
A_1(LO)	225	227	227	228	228
E(TO)	240	238	235	…	…
E(TO)	264	264	263	263	261
E(TO)	278	280	280	281	281
A_1(TO)	306	308	310	309	305
E(TO)	349	347	348	340	332
E(TO)	373	374	375	376	377
E(TO)	439	437	437	437	437
E(LO)	473	475	476	478	482
E(TO)	524	527	529	525	528
A_1(TO)	552	552	552	552	550
E(LO)	612	620	625	618	636

BLFTO ceramics and the corresponding symmetry assignments[24] are given in Table I.

Next, let us concern temperature dependent Raman spectra of BLFTO ceramics. Fig. 2 demonstrates the spectra recorded at several characteristic temperatures and well-fitted deconvolution peaks at 80 K. The spectra of all the samples have the similar variation trend with increasing temperature. The frequencies of the phonon modes shift to low energies and the intensity of all major peaks reduces as the temperature increases from 80 to 680 K. The modes in higher-frequency range become severely widening and merge into a broadening peak. Thermal expansion and thermal disorder, the so-called anharmonic effects of the lattice are responsible for the above observations. In addition, the change of bond length between anions and cations with increasing temperature may also account for the peak shifting.

It is known that any static and/or dynamic changes in the structure should give rise to a variation of the phonon behavior. Therefore, the analysis of the mode position is expected to give insight into those changes. For a closer inspection, the peak positions of E [longitudinal optic (LO)] (78 cm^{-1}), A_1 [transverse optic (TO)] (148 cm^{-1}), and A_1(LO) (173 cm^{-1}) modes are plotted against the temperature between 80 and 300 K, as shown in Fig. 3. Overall, three phonon modes shift to low energies as the temperature increases due to the anharmonic effects of the lattice mentioned. The anharmonic phonon effect is a combined contribution of phonon-phonon and electron-phonon interactions, which play a crucial role in thermal expansion. With increasing temperature, the longitudinal phonons change the interatomic distance along the direction of their propagation, while the transversal modes are perpendicular to their propagation. Additionally, thermally induced disorder effects can perturb the phonon spectra at higher temperatures. Therefore, the dilatation of lattice and thermally induced disorder effects are responsible for the reduction of phonon frequencies. However, the temperature dependence of the frequencies show peaks or troughs around 140 and 205 K, respectively. The noticeable spectral changes have been observed from all the samples. Similar anomalies in the frequencies and intensities of the magnon modes have been reported at 140 and 200 K for BFO.[25] The anomalies in phonon modes suggest a strong magnon-phonon coupling of BLFTO in the present work.

These anomalies have been previously accounted as new magnetic phase transitions at cryogenic temperatures. It was reported that there are spin-reorientation transitions in $RFeO_3$ materials at comparable temperatures.[26] The Fe

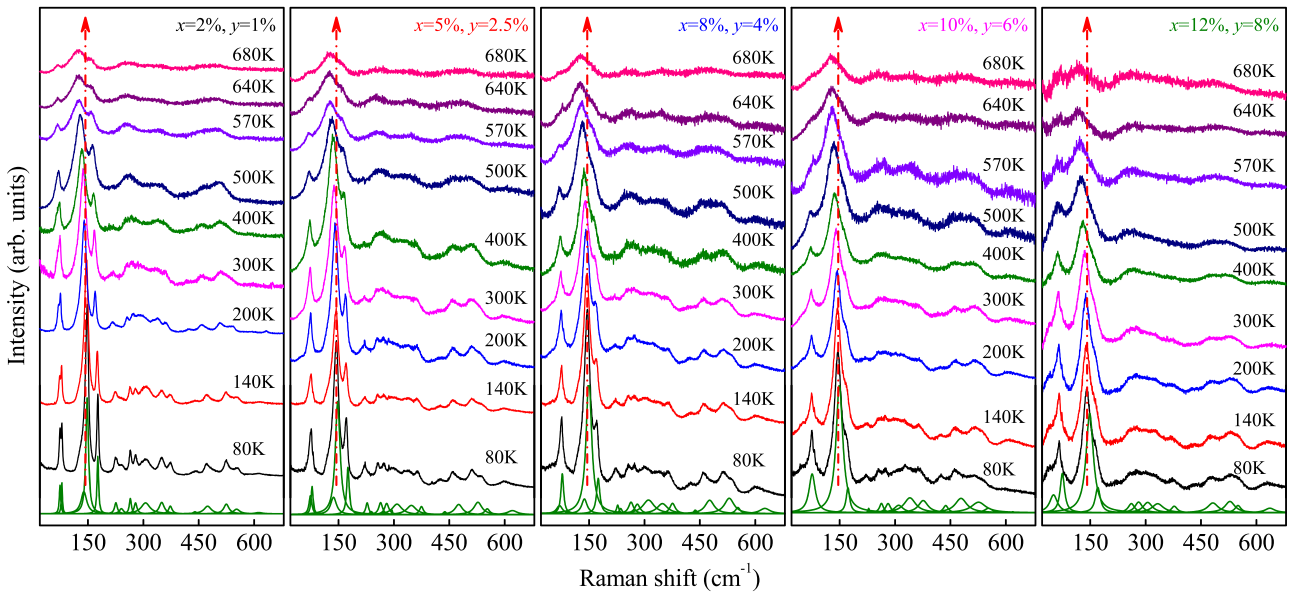

FIG. 2. Temperature dependence of Raman scattering for the BLFTO ceramics collected in the temperature range from 80 to 680 K. As an example, Raman spectra recorded at 80 K, which were fitted with independent damped harmonic oscillators, have been indicated on the bottom. Note that the dashed lines are applied to guide the eyes.

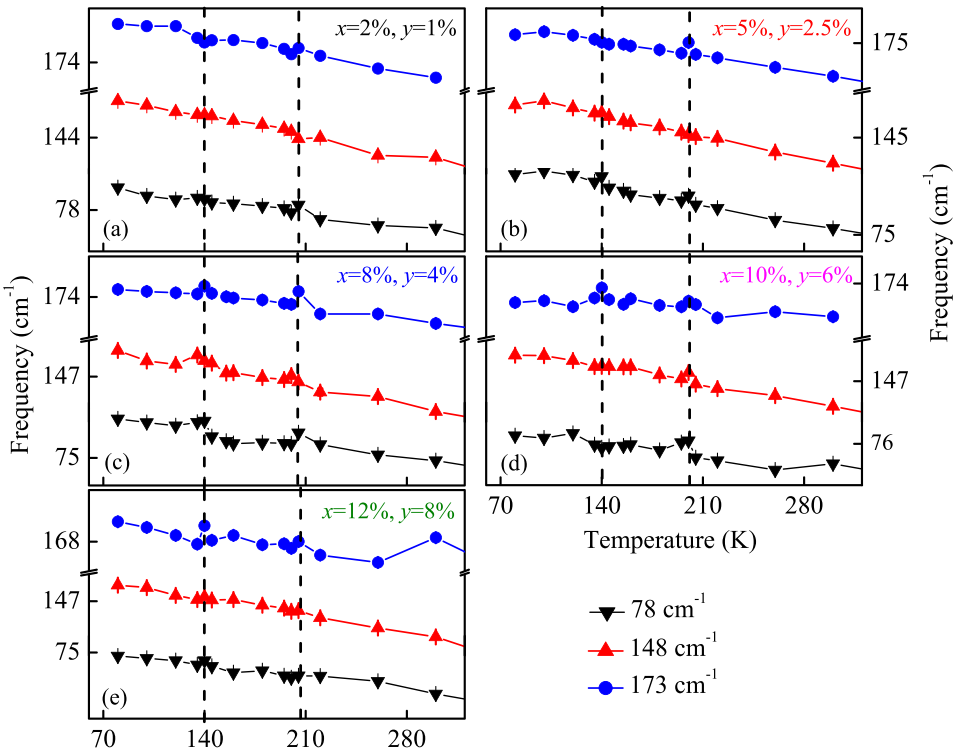

FIG. 3. The frequency variation of three selected Raman modes as a function of temperature for the BLFTO ceramics in the temperature range between 80 and 300 K. Note that the dashed lines indicate the anomalies.

magnetic moments in BLFTO are coupled to the oxygen atoms via the superexchange mechanism. A weak ferromagnetic moment stems from the antisymmetric component of the interaction due to tilting of (Fe, Ti)O_6 octahedra. The magnetic anisotropy is temperature dependent and leads to a spontaneous rotation of the ordered spins within a certain temperature interval, which is called as spin-reorientation transition. Thus, the transition around 140 K can be associated with a spin-reorientation but with slightly coupling to the order parameter. The transition around 205 K shows a strong elastic coupling. It is suggested that a spin glass behavior at low temperature with competition between ferromagnetic and antiferromagnetic may get involved in the unexplained anomaly near 205 K.[27] Moreover, it is proposed that these anomalies around 140 and 200 K indicate a structural rearrangement in local structure and there may be a change in space group.[28] The structural rearrangement in local region cannot be ruled out at cryogenic temperatures. To systematically investigate the phase transitions of the BLFTO ceramics, the peak positions of E(LO) (78 cm^{-1}), A_1(TO) (148 cm^{-1}), and A_1(LO) (173 cm^{-1}) modes are plotted against the temperature from 300 to 680 K, as shown in Fig. 4. The three modes gradually soften with the increase in temperature and show strong anomalies around 570 and 640 K for all doping compositions. It indicates that the anomalies around 570 and 640 K arise from the phase transitions.

The occurrence of the mode at 50 cm^{-1} near the composition of $x = 0.12$, $y = 0.08$ in Fig. 2 indicates that the AFE structure begins to emerge. The AFE structure closely resembles that of the well-established AFE structure in $PbZrO_3$, in which Pb^{3+} is displaced in an anti-parallel manner along the 011 direction. The AFE structure has been previously reported for Dysprosium (Dy)-doped BFO and results from anti-parallel displacements of cations along the [011] direction.[29] It is suggested that the AFE structure belongs to a minority phase. This is consistent with the fact that macroscopic properties of the ceramics agree with those of a ferroelectric rhombohedral phase, even though the AFE structure is observed by means of La and Ti codoping. However, the AFE *Pbam* structure is found to be energetically unfavorable. It is observed only as a minority phase and appears primarily at low doping density before the structural transition takes place in any case. As the temperature increases, the AFE structure gradually disappears, while the orthorhombic phase (*Pnma*) becomes enhanced. On the lower temperature side, the AFE structure is seen as bridge between the rhombohedral phase (*R*3c) and orthorhombic phase (*Pnma*). This intermediate phase results in lattice incommensuration at the rhombohedral-orthorhombic phase boundary.[29] The transition around 570 K is interpreted as a structural transition from rhombohedral (*R*3c) to orthorhombic (*Pnma*) phase because the orthorhombic phase is stable in higher temperature region.

The anomalies around 640 K are ascribed to antiferromagnetic-paramagnetic (AFM-PM) phase transition. BLFTO has a *G*-antiferromagnetic arrangements (*G*-AFM), in which each magnetic atom is surrounded by six antiferromagnetically neighbors. Owing to tilting of (Fe, Ti)O_6 octahedra, the angle of Fe-O-Fe chains is not 180°, which results in canted spin arrangements and further leads to antiferromagnetism with the weak ferromagnetism. The impact of thermal motion gradually increases with increasing temperature. Ultimately, this effect is more evident than that from the exchange interaction between adjacent magnetic moments at T_N, which leads to the collapse of the antiparallel sublattice magnetization of Fe^{3+} and gives rise to spin reorientation of magnetic moments. The anomalies of the

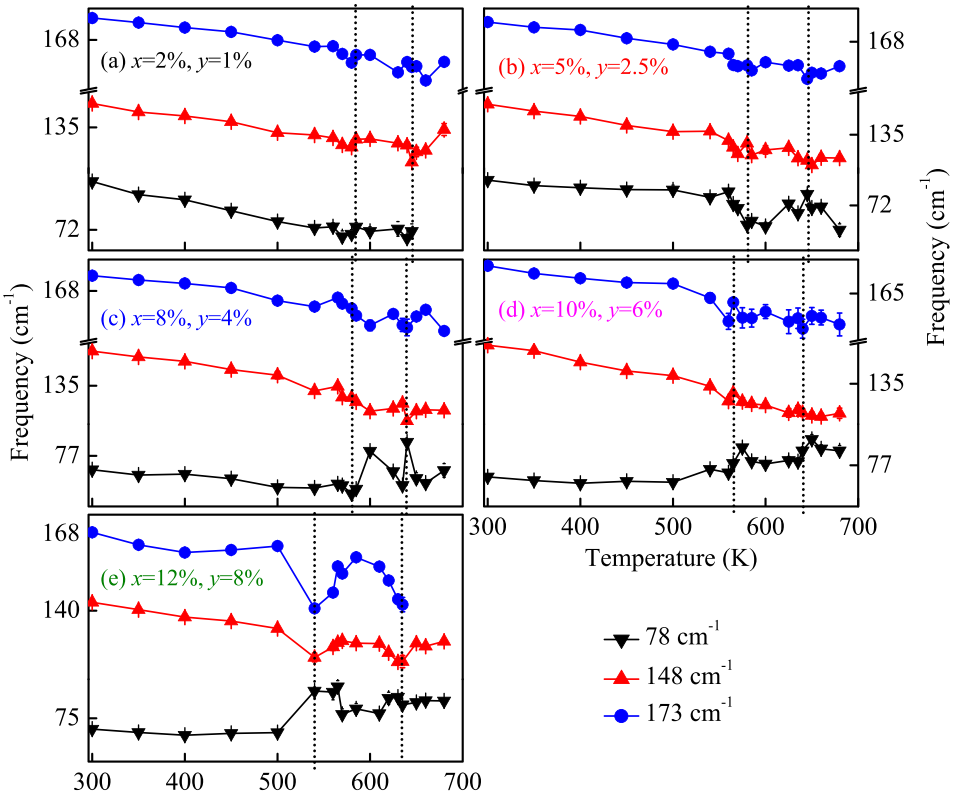

FIG. 4. Temperature dependence of phonon frequency (78, 148, and 173 cm^{-1}) for the BLFTO ceramics at elevated temperatures up to 680 K. Note that the dotted lines show the phase transition temperatures.

phonon modes in the vicinity of T_N may be related to coupling interactions between the spin system and phonons, because the phonon frequencies in multiferroic materials are affected by the correlation of nearest-neighbour spin pairs. However, it is unlikely that the spin-phonon coupling alone can explain the anomalies of the phonon modes. Note that ferroelectric (cation displacement) and ferroelastic (octahedron tilt) instabilities are very sensitive to external perturbations such as temperature, pressure, and stress. The local spin correlations can be regarded as a perturbation. Thus, a further contribution may come from the coupling between magnetic and ferroelectric (and/or ferroelastic) order parameters. It is suggested that the antiferromagnetic transition takes place accompanying with the lattice instabilities.[30] Therefore, the observed anomalies arise from collective actions involving spin-phonon coupling, and spin-charge-lattice coupling.

Fig. 5 shows composition dependence of the local structural transition temperature (T^*) and Néel temperature (T_N). With the increase in the doping compositions of La and Ti, T^* and T_N decrease from 580 to 540 K and from 645 to 630 K, respectively. To obtain insight on the variation trend of T^* and T_N, the influence of the chemical substitution on microstructure should be taken into consideration. The instability in ABO_3 perovskite structure is partly involved in the lattice mismatch between the cations. The mismatch is conveniently quantified in the light of the empirical Goldsmith tolerance factor t, which is closely related to the ionic radii of the A-site, B-site, and O ions, with $t = 1$ corresponding to high stability of the cubic perovskite structure. The t value for BFO is 0.96, in order to minimize the mismatch and gain stability, the cooperative FeO_6 octahedra rotates along the 111 direction. According to La and Ti-codoped in BFO, an external pressure is induced due to size mismatch of host (Bi, Fe) and substitution (La, Ti) cations, which leads to the variation of t and structural distortions. The induced distortions make the rhombohedral phase unstable, but stabilize the orthorhombic phase. Consequently, the average ionic radius r_{ave} of A-site and B-site ions is a critical parameter to describe the structural properties. The variation of r_{ave} increases with increasing doping compositions of La and Ti, which contributes to the decrease of T^*. Moreover, ferroelectricity in BFO depends on the lone-pair polarization of the Bi^{3+} ion, which is absent in La^{3+}. Thus, the parameter T^* decreases with increasing doping compositions of La and Ti elements.

In BFO, the strength of the antiferromagnetic superexchange interaction relies on the Fe-O-Fe angle (θ). Definitely, it is proportional to cos θ. The substitution of Bi by La stretches the lattice and contracts the Fe-O-Fe bond

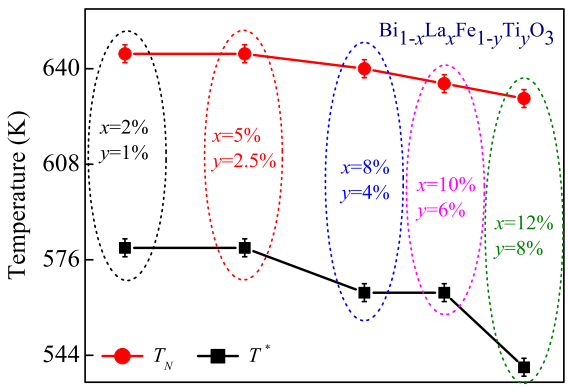

FIG. 5. Composition dependence of phase transition temperature T^* and Néel temperature T_N for the BLFTO ceramics derived from temperature dependent Raman scattering.

angle.[31] These structural effects weaken the magnetic exchange and decrease T_N. In the perovskite structural ferrite, the e_g orbit of *B*-site ions plays a crucial role for T_N.[32] The e_g and t_{2g} orbital overlap integral of *B*-site ions depend on bond angle and bond length between anions and cations in a complex way. In addition, Fe ion substitutions with nonmagnetic Ti^{4+} ions would also reduce the exchange interaction between adjacent magnetic moments. Thus, a complicated mechanism induced by the variation of bond length, bond angle, and the exchange interaction between adjacent magnetic moments could substantially contribute to the shrinking of Néel temperature. Further work is necessary to unambiguously identify the physical mechanisms on the shrinking of T^* and T_N.

IV. SUMMARY

In conclusion, composition dependence of the phonon modes in BLFTO ($0.02 \leq x \leq 0.12$, $0.01 \leq y \leq 0.08$) ceramics has been investigated by Raman scattering in the temperature range from 80 to 680 K. Phonon anomalies have been observed around 140, 205, 570, and 640 K. The anomalies of the phonon frequencies around 140 and 205 K are associated with spin reorientation. The phonon anomalies around 570 K belong to a structural transition from the rhombohedral (*R*3c) to orthorhombic (*Pnma*) phase. The anomalies of the phonon frequencies in the vicinity of T_N may be related to the coupling between magnetic and ferroelectric order parameters and spin-phonon coupling in multiferroic materials. Moreover, the parameters T^* and T_N of BLFTO ceramics decrease with increasing doping compositions of La and Ti.

ACKNOWLEDGMENTS

This work was financially supported by Major State Basic Research Development Program of China (Grant Nos. 2011CB922200 and 2013CB922300), Natural Science Foundation of China (Grant Nos. 11374097 and 61376129), Projects of Science and Technology Commission of Shanghai Municipality (Grant Nos. 14XD1401500, 13JC1402100, and 13JC1404200), and the Program for Professor of Special Appointment (Eastern Scholar) at Shanghai Institutions of Higher Learning.

[1]R. Palai, H. Schmid, J. F. Scott, and R. S. Katiyar, Phys. Rev. B **81**, 064110 (2010).
[2]A. J. Hatt, N. A. Spaldin, and C. Ederer, Phys. Rev. B **81**, 054109 (2010).
[3]S. C. Yang, A. Kumar, V. Petkov, and S. Priya, J. Appl. Phys. **113**, 144101 (2013).
[4]D. V. Karpinsky, I. O. Troyanchuk, V. Sikolenko, V. Efimov, and A. L. Kholkin, J. Appl. Phys. **113**, 187218 (2013).
[5]O. Diéguez, O. E. González-Vázquez, J. C. Wojdeł, and J. Íñiguez, Phys. Rev. B **83**, 094105 (2011).
[6]G. Le. Bras, D. Colson, A. Forget, N. Genand-Riondet, R. Tourbot, and P. Bonville, Phys. Rev. B **80**, 134417 (2009).
[7]D. Lebeugle, D. Colson, A. Forget, M. Viret, P. Bonville, J. F. Marucco, and S. Fusil, Phys. Rev. B **76**, 024116 (2007).
[8]J. Bielecki, P. Svedlindh, D. T. Tibebu, S. Z. Cai, S.-G. Eriksson, L. Börjesson, and C. S. Knee, Phys. Rev. B **86**, 184422 (2012).
[9]G. Catalan and J. F. Scott, Adv. Mater. **21**, 2463 (2009).
[10]C. Ederer and N. A. Spaldin, Phys. Rev. B **71**, 060401(R) (2005).
[11]Y. F. Cui, Y. G. Zhao, L. B. Luo, J. J. Yang, H. Chang, M. H. Zhu, D. Xie, and T. L. Ren, Appl. Phys. Lett. **97**, 222904 (2010).
[12]Z. X. Cheng, X. L. Wang, S. X. Dou, H. Kimura, and K. Ozawa, Phys. Rev. B **77**, 092101 (2008).
[13]Y. Wang and C. W. Nan, Appl. Phys. Lett. **89**, 052903 (2006).
[14]W. Eerenstein, N. D. Mathur, and J. F. Scott, Nature (London) **442**, 759 (2006).
[15]I. O. Troyanchuk, D. V. Karpinsky, M. V. Bushinsky, V. A. Khomchenko, G. N. Kakazei, J. P. Araujo, M. Tovar, V. Sikolenko, V. Efimov, and A. L. Kholkin, Phys. Rev. B **83**, 054109 (2011).
[16]I. Levin, S. Karimi, V. Provenzano, C. L. Dennis, H. Wu, T. P. Comyn, T. J. Stevenson, R. I. Smith, and I. M. Reaney, Phys. Rev. B **81**, 020103(R) (2010).
[17]I. Sosnowska, W. Schäfer, W. Kockelmann, K. H. Andersen, and I. O. Troyanchuk, Appl. Phys. A **74**, 1040 (2002).
[18]V. A. Khomchenko, I. O. Troyanchuk, M. I. Kovetskaya, and J. A. Paixão, J. Appl. Phys. **111**, 014110 (2012).
[19]Y. Y. Liao, Y. W. Li, Z. G. Hu, and J. H. Chu, Appl. Phys. Lett. **100**, 071905 (2012).
[20]X. Chen, Z. G. Hu, Z. H. Duan, X. F. Chen, G. S. Wang, X. L. Dong, and J. H. Chu, J. Appl. Phys. **114**, 043507 (2013).
[21]M. B. Yazdi, K. Y. Choi, D. Wulferding, P. Lemmens, and L. Alff, New J. Phys. **15**, 103032 (2013).
[22]L. P. Xu, L. L. Zhang, P. P. Jiang, J. Yu, Z. H. Duan, Z. G. Hu, Z. Q. Zhu, and J. H. Chu, J. Appl. Phys. **114**, 233509 (2013).
[23]P. Hermet, M. Goffinet, J. Kreisel, and Ph. Ghosez, Phys. Rev. B **75**, 220102(R) (2007).
[24]J. Hlinka, J. Pokorny, S. Karimi, and I. M. Reaney, Phys. Rev. B **83**, 020101(R) (2011).
[25]P. Rovillain, M. Cazayous, Y. Gallais, A. Sacuto, R. P. S. M. Lobo, D. Lebeugle, and D. Colson, Phys. Rev. B **79**, 180411(R) (2009).
[26]S. Venugopalan, M. Dutta, A. K. Ramdas, and J. P. Remeika, Phys. Rev. B **31**, 1490 (1985).
[27]M. K. Singh, R. S. Katiyar, and J. F. Scott, J. Phys.: Condens. Matter **20**, 252203 (2008).
[28]D. Rout, K. S. Moon, and S. J. L. Kang, J. Raman Spectrosc. **40**, 618 (2009).
[29]D. Kan, L. Pálová, V. Anbusathaiah, C. J. Cheng, S. Fujino, V. Nagarajan, K. M. Rabe, and I. Takeuchi, Adv. Funct. Mater. **20**, 1108 (2010).
[30]R. Haumont, J. Kreisel, P. Bouvier, and F. Hippert, Phys. Rev. B **73**, 132101 (2006).
[31]G. Catalan, K. Sardar, N. S. Church, J. F. Scott, R. J. Harrison, and S. A. T. Redfern, Phys. Rev. B **79**, 212415 (2009).
[32]J. B. Goodenough, Phys. Rev. **164**, 785 (1967).